Characterization of the Binding of Deuteroporphyrin IX to the Magnesium Chelatase H Subunit and Spectroscopic Properties of the Complex†

Guy A. Karger, James D. Reid, and C. Neil Hunter*

Robert Hill Institute for Photosynthesis and Krebs Institute for Biomolecular Research, Department of Molecular Biology and Biotechnology, University of Sheffield, Sheffield S10 2TN, U.K.

Received March 20, 2001; Revised Manuscript Received June 8, 2001

ABSTRACT: Magnesium protoporphyrin chelatase catalyzes the insertion of a Mg^{2+} ion into protoporphyrin IX, which can be considered as the first committed step of (bacterio)chlorophyll synthesis. In the present work, the Mg chelatase H subunits from both *Synechocystis* and *Rhodobacter sphaeroides* were studied because of the differing requirements of these organisms for modified cyclic tetrapyrroles. Deuteroporphyrin was shown to be a substrate for Mg chelatase. Analytical HPLC gel filtration was used to show that an H−deuteroporphyrin complex can be reconstituted by incubating the magnesium chelatase H subunit with a molar excess of deuteroporphyrin and that these complexes are monomers. The binding process occurs in the absence of Mg^{2+} or ATP or the I or D subunits of Mg chelatase. The emission from Trp residues in the H subunit is partly quenched when deuteroporphyrin is bound. Quantitative analysis of Trp fluorescence quenching led to determination of the K_d values for deuteroporphyrin binding to BchH from *Rb. sphaeroides* and ChlH from *Synechocystis*, which are 1.22 ± 0.42 μM and 0.53 ± 0.12 μM for ChlH and BchH, respectively. In the case of ChlH, but not BchH, the K_d increased 4-fold in the presence of $MgATP^{2-}$. Red shifts in absorbance and excitation peaks were observed in the B band of the bound porphyrin in comparison with deuteroporphyrin in solution, as well as reduced yield and red shifts of up to 8 nm in fluorescence emission. These alterations are consistent with a slightly deformed nonplanar conformation of the bound porphyrin. Mg deuteroporphyrin, the product of the Mg chelation reaction, was shown to form a complex with either ChlH or BchH; in each case the K_d for Mg deuteroporphyrin is similar to that for deuteroporphyrin. The implications of the H−Mg protoporphyrin interaction for the next enzyme in the chlorophyll biosynthetic pathway, Mg protoporphyrin methyltransferase, are discussed.

Magnesium protoporphyrin IX chelatase catalyzes the insertion of a Mg^{2+} ion into protoporphyrin IX.[1] This reaction can be considered as the first committed step of (bacterio)-chlorophyll synthesis and also as one component of a branch point in tetrapyrrole biosynthesis (*1*). The other component of this branch point involves the insertion of Fe^{2+} into protoporphyrin leading to the formation of heme. Heme and chlorophyll cofactors play a central role in energy transducing complexes, and the redox and light absorbing properties of these tetrapyrroles arise in part from the metal ion present. Thus, the mechanisms governing the insertion of a particular ion and the specificity of this process are both of importance for the assembly and function of energy transducing membranes.

Insertion of Fe^{2+} into protoporphyrin is catalyzed by a ferrochelatase. This enzyme does not require ATP and is a single polypeptide. Recently the structure of the *Bacillus subtilis* enzyme has been determined (*2*,*3*). In contrast, magnesium chelatase consists of three polypeptides, I (36−42 kDa), D (60−74 kDa), and H (130−150 kDa), and the enzyme requires $MgATP^{2-}$ plus free Mg^{2+} ions for activity. The first demonstrations that three proteins comprised the magnesium chelatase employed cell-free extracts of *Escherichia coli* prepared from strains overexpressing the *bch I, D,* and *H* genes from the purple photosynthetic bacterium *Rhodobacter sphaeroides* (*4*) or the *chl I, D,* and *H* genes from the cyanobacterium *Synechocystis* (*5*). Similar approaches were used for the magnesium chelatases of *Chlorobium vibrioforme* and tobacco (*6*, *7*).

Further progress using the purified I, D, and H subunits established optimal conditions for the reaction, in terms of the molar ratios of the subunits, and apparent K_m values for protoporphyrin, Mg^{2+}, and $MgATP^{2-}$ (*8*). Subsequently, it was shown that an I−D−MgATP complex could be purified and that ATP hydrolysis was not necessary for the formation of such a complex (*9*, *10*).

As a result of this work, a reaction scheme was suggested (11): In this scheme (see below) the H subunit is proposed as the protoporphyrin-binding subunit. The first indication of such a role for the H subunit arose from the observation that an *E. coli* strain overproducing BchH from

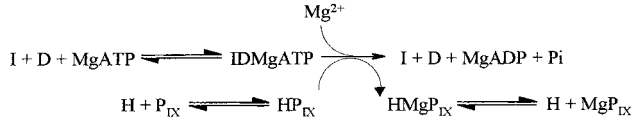

† This work was funded by the Biotechnology and Biological Sciences Research Council of the U.K.

* Corresponding author. E-mail: C.N.Hunter@sheffield.ac.uk. Tel.: +44 114 222 4191. Fax: +44 114 272 8697.

[1] Abbreviations: Mg, magnesium; *Rb. sphaeroides*, *Rhodobacter sphaeroides; Synechocystis*, *Synechocystis PCC 6803; Trp, tryptophan;* V_0, void volume.

10.1021/bi010562a CCC: $20.00 © 2001 American Chemical Society
Published on Web 07/14/2001

Rb. sphaeroides exhibited a noticeable red color attributable to protoporphyrin (*4*). It was also observed that, in continuous assays of Mg chelatase activity, preincubation of ChlH with protoporphyrin shortened the lag period which precedes product formation (*8*). If the role of the H subunit is to bind protoporphyrin prior to insertion of Mg^{2+}, this would have important consequences for the catalytic mechanism and also for the amount of protoporphyrin available at the branch point for ferrochelatase. Indeed partitioning of protoporphyrin between these branches (*12*) could be governed by the H−protoporphyrin interaction (*13*). Such a regulatory role for the Mg chelatase H subunit would have important implications for the way in which fluxes through the heme and chlorophyll pathways are controlled. It is likely that the importance of the H subunit is more widespread; recent studies of the GUN5 mutant of *Arabidopsis thaliana* lead to the conclusion that the Mg chelatase H subunit is involved in signal transduction between the plastid and the nucleus (*14*). Such work underlines the importance of obtaining a quantitative understanding of how porphyrin binds to H and how catalysis of Mg^{2+} chelation proceeds.

The Mg chelatase H subunits from both *Synechocystis* and *Rb. sphaeroides* provide an interesting contrast because of the differing tetrapyrrole requirements of these organisms. In S*ynechocystis* the flux down the Fe^{2+} branch of tetrapyrrole biosynthesis is expected to be far more significant than in *Rhodobacter*. In the cyanobacteria heme is required for cytochromes but also as a source of the linear tetrapyrroles which are used as light-harvesting pigments in the phycobilisomes (*15*). In the purple photosynthetic bacteria and in plants, the chlorophyll (Mg^{2+}) branch dominates because the photosystems rely on chlorophylls for both antenna and photochemical complexes. A comparison of the Mg chelatase H subunits from *Synechocystis* and *Rhodobacter* could therefore reveal interesting differences in the protoporphyrin binding properties of these proteins, with consequences for both the functional and regulatory roles of these subunits.

To obtain more detailed information on the catalytic mechanism of Mg chelatase, it is necessary to study the partial reactions in detail. Thus, the interactions between protoporphyrin and H, and also those between I, D, and $MgATP^{2-}$, require separate study. In the present work it has been established that deuteroporphyrin, more water-soluble than protoporphyrin, is a substrate for Mg chelatase. The associations between the H subunit and deuteroporphyrin have been examined in the present study using analytical HPLC gel filtration, which has established that an H−deuteroporphyrin complex can be isolated. The emission from Trp residues in the H subunit is partly quenched when either deuteroporphyrin or Mg deuteroporphyrin is bound; quantitative analysis of this quenching has allowed us to determine the K_d values for binding of these porphyrins to BchH from *Rb. sphaeroides* and ChlH from *Synechocystis*. Alterations in absorbance and fluorescence properties of deuteroporphyrin in upon binding to the H subunit are consistent with a slightly deformed nonplanar conformation of the bound porphyrin. These data enabled us to assess the properties of the H−deuteroporphyrin and H−Mg−deuteroporphyrin complexes that could arise during steady-state catalysis of Mg^{2+} insertion.

EXPERIMENTAL PROCEDURES

Protein Production and Purification. The plasmids pET9a-ChlH (*5*) and pET14b-BchH (*10*) were each transformed into *E. coli* BL21(DE3) cells, and expression of recombinant proteins was performed as described in refs *4* and *5*. Purification of the ChlH and BchH proteins was performed essentially as described in refs *8* and *10*.

After purification, BchH from *Rb. sphaeroides* appears red due to endogenously bound protoporphyrin. The molar ratio of protoporphyrin: BchH is typically 1:5 (20%). For the quantitative analysis described in this paper it was necessary to "strip" the bound protoporphyrin from BchH beforehand. The purified protein was applied to a Ni^{2+} agarose affinity column according to the manufacturer's instructions (Novagen) and, after the binding step, was washed with 6 column volumes of wash buffer (20 mM Tris-HCl, pH 7.9, 60 mM imidazole, 1 M NaCl, and 0.5% Tween-20). Protein was recovered by elution with imidazole buffer (20 mM Tris-HCl, pH 7.9, 500 mM imidazole, 0.5 M NaCl); pooled fractions were dialyzed first into 50 mM Tricine-NaOH, pH 7.9, 1 M NaCl, and 0.5% Tween-20 and subsequently into 50 mM Tricine-NaOH, pH 7.9, 50% (v/v) glycerol, and 1 mM DTT and stored at −70 °C. The stripped BchH, which retained full activity in Mg chelatase assays, had a molar ratio of protoporphyrin:BchH of 1:20 (5%). In contrast, no stripping procedure was necessary for the *Synechocystis* H subunit (ChlH): when purified the ChlH was almost free from bound porphyrin, with a molar ratio of protoporphyrin: BchH of 1:30 (3%).

Analytical Gel Filtration by HPLC. A Shodex KW-803 column was equilibrated with running buffer consisting of 50 mM MOPS/KOH, pH 7.7 (50 mM Tricine/KOH, pH 7.9, for BchH experiments), 100 mM NaCl, 300 mM glycerol, and 1 mM DTT at 1.0 mL min^{-1}. The column was calibrated with the following markers: blue dextran (V_0); thyroglobulin (669 kDa); sweet-potato β-amylase (200 kDa); yeast alcohol dehydrogenase (150 kDa); bovine erythrocyte carbonic anhydrase (29 kDa).

A 1 μM concentration of ChlH or BchH was incubated in the presence or absence of 48 μM deuteroporphyrin, 5 mM ATP, and 10 mM $MgCl_2$ in running buffer for 5 min at 34 °C. Samples were analyzed by loading 20 μL aliquots onto the column and following elution by recording either protein fluorescence at 350 nm (excitation at 280 nm) or deuteroporphyrin fluorescence at 615 nm (excitation at 390 nm). Protein absorbance scans were taken simultaneously in order to obtain estimates of total protein concentration, because of variable fluorescence yields at 350 nm.

Spectroscopy. Fluorescence spectra were recorded on a SPEX Fluorolog spectrofluorometer fitted with a temperature-controlled cuvette holder set to 34 °C. For composition of samples, see legends to Figures 2−4. All ChlH samples were in 50 mM MOPS-KOH, pH 7.7, 300 mM glycerol, and 1 mM DTT while all BchH samples were in 50 mM Tricine-KOH, pH 7.9, 300 mM glycerol, and 1 mM DTT. Samples (1 mL) were incubated for at least 5 min at 34 °C before transfer to a Starna semi-micro quartz cuvette. For protein fluorescence emission measurements at 350 nm, excitation wavelengths of 280 nm (when no ATP was present) and 295 nm (when ATP was present) were chosen. Excitation and emission slit widths corresponding to 4.5 and

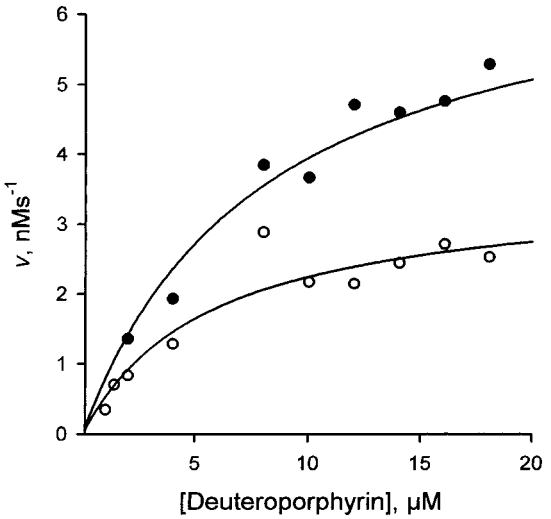

FIGURE 1: Dependence of steady-state rate (v) of magnesium chelation on deuteroporphyrin concentration at 37 °C, I 0.1 M, pH 7.7, with 0.5 μM ChlD, 1 μM ChlI, 5 mM $MgATP^{2-}$, 5 mM Mg^{2+}, and 0.1 μM ChlH (○) or 0.2 μM ChlH (●). The lines are theoretical for a Michelis−Menten rate equation with the following parameter values, determined by nonlinear regression analysis weighted by the constant absolute error condition: upper line (200 nM ChlH), $V_{max} = 7 \pm 0.5$ nM s^{-1}, $K_m = 8 \pm 1.6$ μM; lower line (100 nM ChlH), $V_{max} = 3.5 \pm 0.33$ nM s^{-1}, $K_m = 5.7 \pm 1.7$ μM.

18 nm, respectively, were used for excitation scans. For emission scans both slits were set at 4.5 nm. Other excitation and emission wavelengths used are quoted in the legends to Figures 6 and 7.

Absorbance spectra were recorded on a Beckman DU 640 spectrophotometer. The buffers used were the same as for fluorescence spectroscopy.

Stock porphyrin solutions were prepared by dissolving a small amount of porphyrin in buffer. These solutions aggregated after 2−3 weeks storage at −20 °C when they became visibly turbid; fresh solutions were prepared weekly. Porphyrin concentrations were determined in 0.1 M HCl using the ϵ_{398} of 433 000 M^{-1} cm^{-1}, magnesium deuteroporphyrin IX having been converted to deuteroporphyrin IX by a 5 min incubation in 1 M acetic acid.

Analysis of Apparent Disassociation Constants for Deuteroporphyrin and Mg Deuteroporphyrin with ChlH and BchH. Binding titration data were fitted to eq 1, in which a single type of binding site is assumed:

$$F_{obs} = F_0 + F_{max}\frac{[L]_T + [E]_T + K_d - \sqrt{([L]_T + [E]_T + K_d)^2 - 4[L]_T[E]_T}}{2[E]_T} \quad (1)$$

where F_{obs} is the observed fluorescence, F_0 is initial fluorescence, F_{max} is the maximum amplitude of fluorescence quenching, $[L]_T$ is the total ligand concentration, $[E]_T$ is the total concentration of H protein (fixed at 0.1 μM during the fitting procedure), and K_d is the apparent disassociation constant.

Magnesium Chelatase Assays. Reactions were carried out at 34 °C in 50 mM MOPS/KOH, I 0.1, 1 mM DTT, pH 7.7, in a Bio-Tek F2 microplate reader with excitation through a 420 ± 25 nm filter and emission observed through a 590 ± 17.5 nm filter. Protein concentrations were 0.5 μM ChlD, 1 μM ChlI, and 0.1 or 0.2 μM ChlH, and substrate concentrations were 5 mM $MgATP^{2-}$, 5 mM Mg^{2+}, and 1 or 2 to 20 μM deuteroporphyrin IX. Observed fluorescence was linear within this range of porphyrin concentration. The maximum rate during an assay was taken as the steady-state rate and generally occurred after a 10 min lag phase.

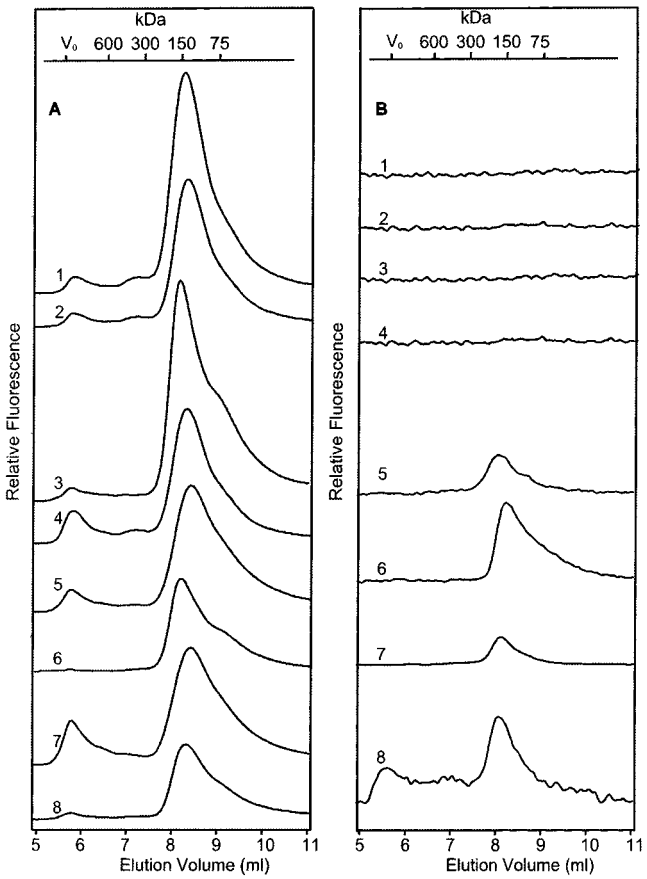

FIGURE 2: Gel filtration chromatograms of ChlH. Samples containing 1 μM H protein were incubated with or without 48 μM deuteroporphyrin, 5 mM ATP, and 10 mM $MgCl_2$ for 30 min at 34 °C and applied to an HPLC gel filtration column preequilibrated with buffer and calibrated using the following markers: blue dextran (V_0); thyroglobulin (669 kDa); β-amylase (200 kDa); alcohol dehydrogenase (150 kDa); cytochrome c oxidase (29 kDa). (A) Protein fluorescence chromatograms. (B) Deuteroporphyrin fluorescence chromatograms. Key: 1, ChlH; 2, ChlH and $MgCl_2$; 3, ChlH and ATP; 4, ChlH, $MgCl_2$, and ATP; 5, ChlH and deuteroporphyrin; 6, ChlH, deuteroporphyrin, and $MgCl_2$; 7, ChlH, deuteroporphyrin, and ATP; 8, ChlH, deuteroporphyrin, $MgCl_2$, and ATP. The chromatograms in B have been normalized to the absorbance at 280 nm.

RESULTS

Steady-State Kinetics of Magnesium Chelatase: Assessment of an Apparent K_m for Deuteroporphyrin. Previous work on steady-state kinetics of the magnesium chelatases from *Synechocystis* and *Rb. sphaeroides* had concentrated on the biological substrate, protoporphyrin (*8*−*11*); working with this porphyrin however in aqueous solution requires the presence of detergent (Tween 80), in contrast with the relatively soluble analogue deuteroporphyrin that lacks the two vinyl groups on the A and B rings. The present work describes the use of the more water-soluble deuteroporphyrin, which greatly simplifies the work described in this paper.

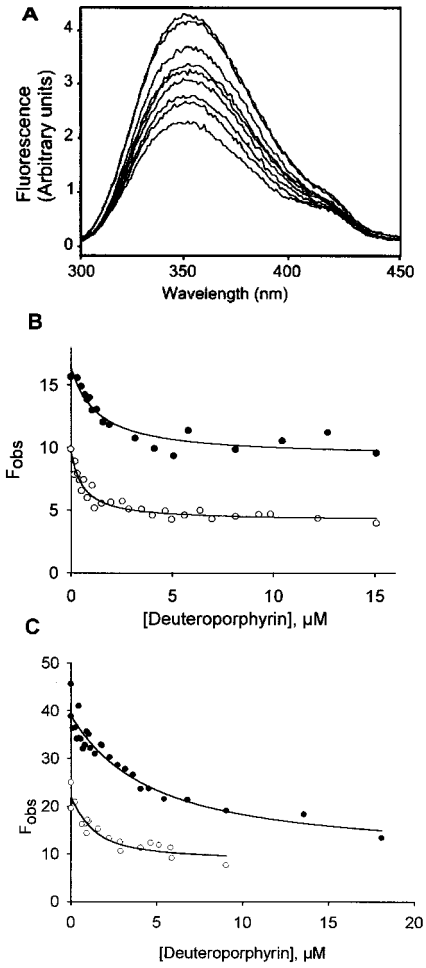

FIGURE 3: Quenching of Mg chelatase H subunit protein fluorescence by deuteroporphyrin. The 0.1 μM purified H protein was incubated with 0−18 μM deuteroporphyrin for 5 min at 34 °C. (A) Fluorescence emission scans were recorded at 34 °C with an excitation wavelength of 280 nm (295 nm when $MgCl_2$ and ATP were included in the assay). A series of spectra showing quenching of ChlH fluorescence by deuteroporphyrin in the absence of $MgCl_2$ and ATP are shown. (B) Plots of ChlH (●) and BchH (○) fluorescence against deuteroporphyrin concentration were recorded. The lines are described by a single-site binding model (eq 1) with K_d values for deuteroporphyrin binding of 1.22 ± 0.42 and 0.53 ± 0.12 μM, respectively. (C) Plots of ChlH (●) and BchH (○) fluorescence against deuteroporphyrin concentration in the presence of 5mM ATP and 10 mM $MgCl_2$ were recorded. The lines are described by a single-site binding model with a K_d for deuteroporphyrin of 4.00 ± 1.30 and 0.75 ± 0.42 μM, respectively.

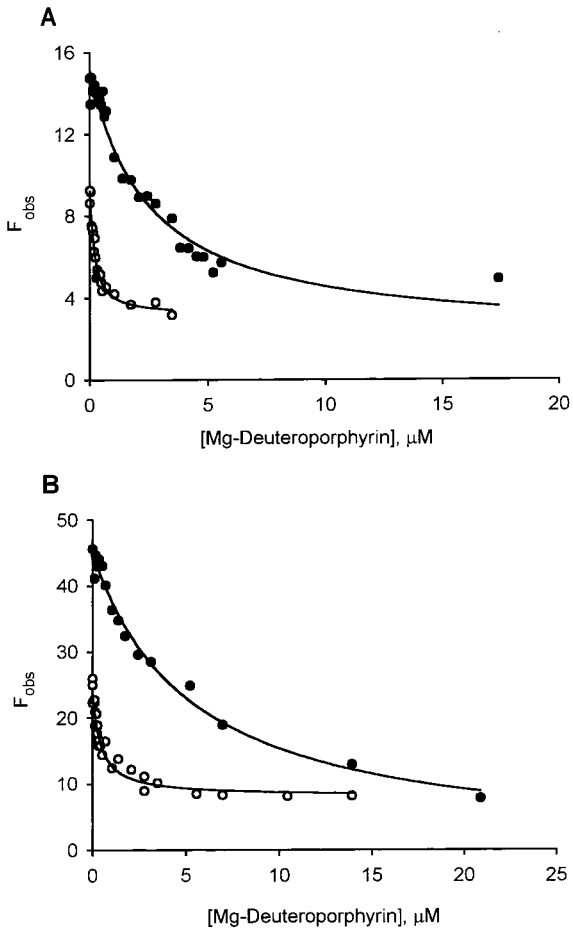

FIGURE 4: Quenching of Mg chelatase H subunit protein fluorescence by Mg−deuteroporphyrin. The 0.1 μM of purified H protein was incubated with 0−21 μM Mg−deuteroporphyrin for at least 5 min at 34 °C. (A) Fluorescence emission scans were recorded at room temperature with an excitation wavelength of 280 nm (295 nm when $MgCl_2$ and ATP were included in the assay). A series of spectra showing quenching of ChlH fluorescence by Mg−deuteroporphyrin in the absence of $MgCl_2$ and ATP are shown. (B) Plots of ChlH (●) and BchH (○) fluorescence against Mg−deuteroporphyrin concentration were recorded. The lines are described by a single-site binding model with K_d values for Mg−deuteroporphyrin binding of 2.43 ± 0.46 and 0.22 ± 0.038 μM, respectively. (C) Plots of ChlH (●) and BchH (○) fluorescence against Mg−deuteroporphyrin concentration in the presence of 5 mM ATP and 10 mM $MgCl_2$. The data fit eq 1, giving K_d values for Mg−deuterporphyrin binding of 5.24 ± 0.84 and 0.16 ± 0.03 μM, respectively.

Therefore, it was necessary to determine whether deuteroporphyrin is a substrate for Mg chelatase, especially in view of the report that deuteroporphyrin cannot act as substrate for the *Rb. capsulatus* enzyme (*16*). The dependence of initial rate of Mg chelation on deuteroporphyrin concentration was determined for the *Synechocystis* enzyme, using purified H, I, and D subunits. The deuteroporphyrin kinetics in Figure 1 demonstrate a simple hyperbolic dependence of rate (v) upon porphyrin concentration ($V_{max}/[H]_{total} = 0.0350 \pm 0.003$ s^{-1}; $K_m = 8 \pm 1.6$ μM). Inhibition at high substrate concentrations was not seen, unlike that seen with protoporphyrin (*8*), where inhibition occurs at greater than 1 μM substrate. We propose that the previously observed inhibition does not reflect an additional porphyrin binding site but is probably due to an aggregation of protoporphyrin, as suggested previously (*8*), or to partitioning between detergent micelles (Tween 80 is required to help solubilize protoporphyrin) and enzyme active sites. The availability of a water-soluble porphyrin substrate for this magnesium chelatase will greatly simplify future kinetic analyses.

Analytical Gel Filtration of H−Porphyrin Complexes. Analytical gel filtration was used to examine the association between deuteroporphyrin and the Mg chelatase H subunits from *Synechocystis* and *Rb. sphaeroides* using HPLC. The ChlH and BchH proteins (1 μM) were incubated with combinations of 48 μM deuteroporphyrin, 5 mM ATP, and 10 mM Mg^{2+} for 5 min at 34 °C and then applied to a calibrated HPLC gel filtration column. Chromatograms were obtained arising from both protein (excitation 280 nm, emission detection 350 nm) and deuteroporphyrin (excitation 390 nm, emission detection 615 nm). Successive experiments provided comparisons between the effects of ATP, Mg^{2+},

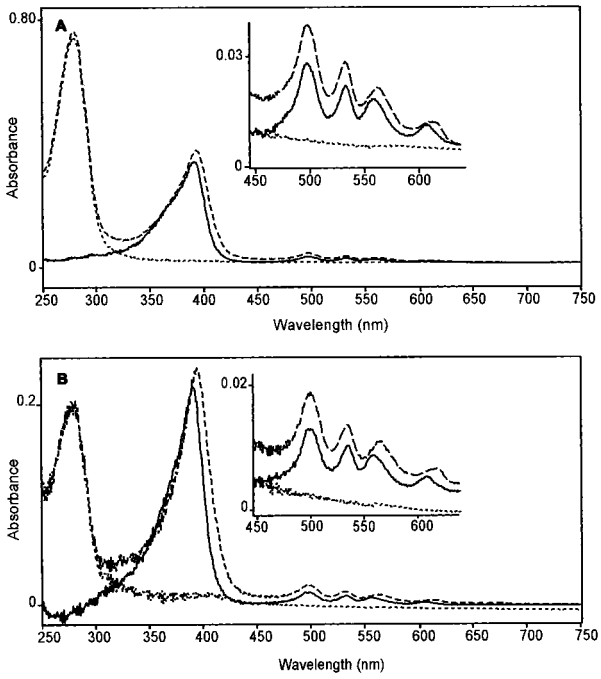

FIGURE 5: UV−visible absorbance spectra of ChlH−deuteroporphyrin and BchH−deuteroporphyrin complexes: (A) absorbance spectra of 4 μM ChlH (dotted line), 4 μM deuteroporphyrin (solid line), 4 μM ChlH, and 4 μM deuteroporphyrin (dashed line); (B) absorbance spectra of 2 μM BchH (dotted line), 2 μM deuteroporphyrin (solid line), 2 μM BchH, and 2 μM deuteroporphyrin (dashed line). The inserts in (A) and (B) show expanded spectra in the 450−620 nm region. Samples were incubated at 34 °C for 5 min prior to measurement.

and the mixture of the two on the H−deuteroporphyrin interaction and on the apparent molecular mass of the H protein.

With no added deuteroporphyrin, ChlH elutes as a peak corresponding to 148 kDa (Figure 2A, trace 1). Given the predicted molecular mass from the primary sequence of 151 kDa, this indicates the presence of a monomer. Preincubation of ChlH with ATP, Mg^{2+}, or ATP and Mg^{2+} together (Figure 2A, traces 2−4) had little effect on the elution position, although the combination of ATP and Mg^{2+} (Figure 2A, trace 4) promoted the appearance of a small proportion of aggregated forms of ChlH possibly corresponding to tetramers (~646 kDa) and higher aggregation states (>700 kDa). When ChlH is preincubated with deuteroporphyrin (Figure 2A, traces 5−8) the major protein peak again corresponded to H monomers. The presence of ATP in the preincubation along with deuteroporphyrin was the most effective in promoting higher aggregation states. An asymmetry of the elution profiles was observed at longer elution times. The protein preparations used for this work were pure, giving only a single band in SDS−PAGE (not shown), so the elution profiles cannot be explained by impurities of lower molecular mass than ChlH. The profiles could have arisen by the H protein deviating from nonideal behavior due to interaction with the column.

Chromatograms of the same samples as in Figure 2A were also obtained by monitoring fluorescence emission from deuteroporphyrin at 615 nm (Figure 2B, traces 5−8). This specifically detects those H proteins that have bound deuteroporphyrin. The elution profiles in Figure 2B, traces 1−4, indicate that no detectable porphyrin had remained bound

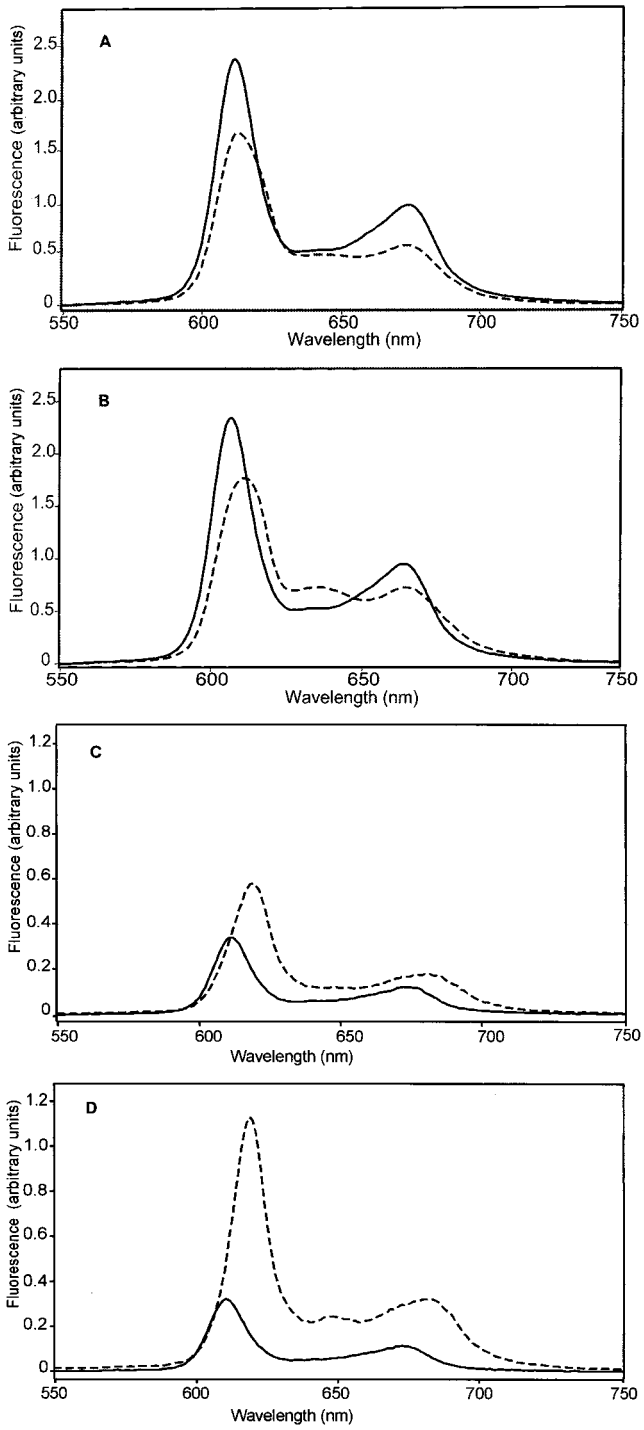

FIGURE 6: Fluorescence emission spectra of ChlH−deuteroporphyrin and BchH−deuteroporphyrin complexes. Scans were recorded at 34 °C with excitation wavelengths of either 390 nm (A, B) or 280 nm (C, D): (A, C) 4 μM deuteroporphyrin (solid line), 4 μM deuteroporphyrin, 4 μM ChlH (dashed line); (B, D) 4 μM deuteroporphyrin (solid line), 4 μM deuteroporphyrin, 4 μM BchH (dashed line).

to ChlH during the purification procedure. Traces 5−8 show that preincubation with deuteroporphyrin was effective in producing a porphyrin−H complex. Preincubation of a ChlH−deuteroporphyrin mixture with Mg^{2+} or ATP and Mg^{2+} together (Figure 2B, traces 6 and 8) has increased the amount of porphyrin bound to H; these peaks correspond to an apparent molecular mass of approximately 150 kDa, in agreement with the data obtained from detection of protein

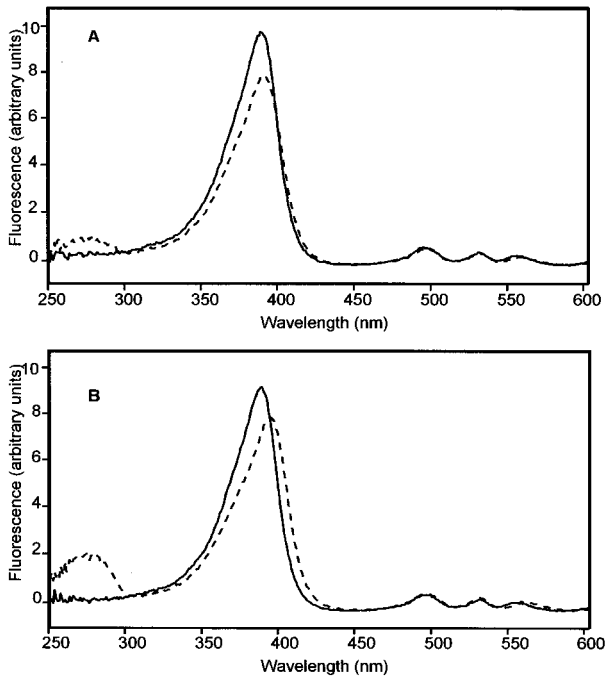

FIGURE 7: Fluorescence excitation spectra of ChlH−deuteroporphyrin and BchH−deuteroporphyrin complexes: (A) excitation spectra (detection of emission at 613 nm) of 4 μM deuteroporphyrin (solid line), 4 μM ChlH, 4 μM deuteroporphyrin (dashed line); (B) excitation spectra (detection of emission at 613 nm) of 4 μM deuteroporphyrin (solid line), 4 μM BchH, 4 μM deuteroporphyrin (dashed line). Scans were recorded at 34 °C.

fluorescence in Figure 2A. This suggests that the ChlH−deuteroporphyrin complex is a monomer. No quantitative comparisons can be made from these data, since the amounts of protein fluorescence recorded in Figure 2A are attenuated by binding of deuteroporphyrin, and vice-versa, as can be seen in subsequent figures. However, the absorbance of all samples had been continuously monitored at 280 nm, which gives a rough idea of the amount of protein present. The absorbance values were normalized for the peaks in traces 5−8 in Figure 2B, and so it appears likely that Mg^{2+} in particular enhances amount of deuteroporphyrin that forms a complex with ChlH.

The data for BchH were broadly similar to those for ChlH (not shown). BchH migrates as a monomer, judging by the peak corresponding to an apparent molecular mass of 110 kDa. The apparent molecular mass for a monomer predicted from the primary sequence is slightly smaller than for ChlH, at 130 kDa. Fluorescence detection at 615 nm demonstrated that deuteroporphyrin comigrates with the BchH protein, as found for ChlH.

In summary, analytical gel filtration shows that a complex can be reconstituted by incubating the magnesium chelatase H subunit with a molar excess of deuteroporphyrin. The binding process occurs in the absence of Mg^{2+} or ATP or the I or D subunits of Mg chelatase. H−deuteroporphyrin complexes are monomeric under the conditions tested. Under the conditions used for HPLC analysis, it is likely that the majority of the protein has not formed such a complex, but specific detection of deuteroporphyrin fluorescence reveals a population of monomeric H−deuteroporphyrin complexes. These data are consistent with the designation of the H subunit as the porphyrin-binding subunit of Mg chelatase.

Determination of Apparent Dissociation Constants for Deuteroporphyrin and Mg Deuteroporphyrin with ChlH and BchH. The data in Figure 2 emphasized the need for quantitative analyses of the binding of deuteroporphyrin to ChlH and BchH. Deuteroporphyrin was preferred over protoporphyrin for this work as this avoided the use of detergents for solubilization and consequent concentration-dependent aggregation, which affect the absorbance and emission properties of this pigment.

With excitation at 280 nm, emission of fluorescence from the H subunit was recorded from 300 to 500 nm. A typical family of spectra is shown in Figure 3A, in which 0−18 μM deuteroporphyrin was added to 0.1 μM ChlH. The addition of ligand was accompanied by a progressive quenching of protein fluorescence at 350 nm (Figure 3A). Figure 3B displays plots of integrated fluorescence from ChlH and BchH as a function of deuteroporphyrin concentration. In each case, it was found that the curve fits a single-site binding model and K_d values of 1.22 ± 0.42 μM and 0.53 ± 0.12 μM were obtained for ChlH and BchH, respectively. To assess if the fits for the data could be improved by a two-site binding model, they were fitted numerically using DYNAFIT (*17*). No improvement in the residual plots was seen, and parameter values for the second site were beyond the data range with large standard errors. We therefore conclude that the data can be explained by a single type of binding site. These experiments were repeated in the presence of 5 mM ATP and 10 mM $MgCl_2$, essentially 5 mM $MgATP^{2-}$ and 5 mM Mg^{2+} (Figure 3C). Again, the data fit a single-site binding model with K_d values of 4.00 ± 1.30 and 0.75 ± 0.41 μM for ChlH and BchH, respectively.

Finally, the experiments were carried out using Mg deuteroporphyrin as the ligand. This is a product of the Mg chelatase reaction, and it was of interest to see if Mg deuteroporphyrin could form a complex with either H protein. Experiments analogous to those in Figure 3 were therefore performed using Mg deuteroporphyrin IX instead of deuteroporphyrin IX. Again, quenching of Trp fluorescence from ChlH and BchH was observed upon addition of Mg deuteroporphyrin and quantitative analyses of this quenching, without and with 5 mM ATP and 10 mM $MgCl_2$, are shown in Figure 4A,B. The data fit eq 1 with K_d values for Mg−deuteroporphyrin binding of 2.43 ± 0.46 and 0.22 ± 0.04 μM for ChlH and BchH, respectively (Figure 4A). K_d values of 5.24 ± 0.84 and 0.16 ± 0.03 μM were obtained for Mg−deuteroporphyrin binding to ChlH and BchH, respectively, in the presence of 5 mM ATP and 10 mM $MgCl_2$ (Figure 4B).

Spectroscopic Studies of H−Deuteroporphyrin Complexes. The determination of K_d values in the previous section allowed conditions to be chosen for spectroscopy which favored the formation of H−deuteroporphyrin complexes. A series of absorbance, fluorescence excitation, and emission spectra were recorded, to investigate whether the properties of deuteroporphyrin were altered in the protein-bound state.

Figure 5 displays the absorbance spectra of deuteroporphyrin in solution (solid lines), the spectra of both ChlH and BchH (dotted lines), and an equimolar combination of the two, at a concentration (2 or 4 μM) that allows both of the complexes to form (dashed lines). The absorbance spectra revealed differences in the absorbance of deuteroporphyrin

in the presence of ChlH or BchH; in each case the B (Soret) band and the two redmost Q-bands were slightly broadened and red-shifted upon addition of the H subunit. In Figure 5A, the B band of deuteroporphyrin is shifted by 2 nm in the presence of ChlH, and in Figure 5B, the shift with BchH is 4 nm. The shifts for the two redmost Q-bands were 4 and 5 nm and 6 and 9 nm respectively for ChlH−deuteroporphyrin and BchH−deuteroporphyrin.

The fluorescence emission spectra of equimolar (4 μM) ChlH/deuteroporphyrin and BchH/deuteroporphyrin mixtures are displayed in Figure 6A,B, with excitation of the B band of the porphyrin at 390 nm. When ChlH or BchH was added both emission peaks of deuteroporphyrin at 615 and 670 nm were quenched and the major (615 nm) peak was red-shifted by 2 and 7 nm for ChlH and BchH, respectively. A third emission peak at 639 nm was particularly noticeable for the BchH−deuteroporphyrin complex. Another set of emission spectra were recorded with the same samples, this time with 280 nm excitation (Figure 6C,D). Excitation at this wavelength tends to select those deuteroporphyrin molecules in the protein-bound state, making any resulting alterations in emission easier to detect. Excitation at 280 nm, into the blue tail of the excitation maximum at 389 nm (see Figure 7), elicits fluorescence from deuteroporphyrin (solid lines). When either of the H proteins is present, two changes occur. First, the emission shifts to the red, consistent with the shifts seen in Figure 6A,B and with the idea that in the protein-bound state the emission properties of deuteroporphyrin have been altered. Second, there is an increased yield of fluorescence, particularly marked in the case of BchH−deuteroporphyrin (Figure 6D), which could arise from excitation of the protein, and subsequent energy transfer to the bound porphyrin. This is particularly true for BchH, since it has a lower K_d for deuteroporphyrin than does ChlH, and so more of this ligand is in the bound state. To examine this further, excitation spectra were recorded.

The excitation spectra for the same samples as in Figure 6 are displayed in Figure 7. With detection of porphyrin emission at 613 nm an excitation peak at 389 nm was obtained for free deuteroporphyrin, whereas in the 4 μM ChlH/deuteroporphyrin and BchH/deuteroporphyrin mixtures this had shifted to 392 and 395 nm, respectively.

These red shifts in the 390 nm region mirror the changes seen in the absorbance spectra in Figure 5. Also visible for each protein−porphyrin mixture is a small excitation peak at 280 nm, arising from energy transfer from aromatic residues in the H protein to the bound porphyrin. The larger excitation peak for BchH−deuteroporphyrin (Figure 7B) is consistent with the greater enhancement of deuteroporphyrin emission seen for the BchH−deuteroporphyrin complex (Figure 6D) when compared to the ChlH−deuteroporphyrin complex (Figure 6C), with excitation at 280 nm.

DISCUSSION

Deuteroporphyrin is relatively water-soluble in comparison with the biological substrate for Mg chelatase, protoporphyrin. The use of deuteroporphyrin for the work described above has enabled us to examine the interactions between the H subunits of the magnesium chelatases from *Synechocystis* and *Rb. sphaeroides* with porphyrin in some detail. The steady-state kinetic data in Figure 1 were obtained to establish that deuteroporphyrin is a substrate for Mg chelatase, especially in view of the report that deuteroporphyrin cannot act as substrate for the *R. capsulatus* enzyme (*16*). Given the difficulties in working with porphyrins in aqueous media (*18*), this apparent inability of deuteroporphyrin to act as substrate could reflect the poor solubility of deuteroporphyrin in the buffer system used (*16*).

Formation of an H−Deuteroporphyrin Complex: Qualitative and Quantitative Analyses of the Effects on the Mg Chelatase H Subunit. The analytical gel filtration experiments in Figure 2 show that ChlH of *Synechocystis* and BchH from *Rb. sphaeroides* are monomeric, whether the majority of protein has a bound porphyrin. A complex can be reconstituted by incubating either magnesium chelatase H subunit with a molar excess of deuteroporphyrin. Since these are not equilibrium measurements, most of the H proteins that elute are unlikely to be in the ligand-bound state, and therefore, the elution profiles in Figure 2A are presumed to reflect the behavior of the bulk of H, which is free of porphyrin. Specific detection of the H−deuteroporphyrin complexes using porphyrin fluorescence reveals that they have the same mobility in the column as the porphyrin-free protein.

Porphyrin binding occurs in the absence of the I or D subunits of Mg chelatase. An interesting and useful feature of deuteroporphyrin binding is that it results in partial quenching of Trp fluorescence in ChlH and BchH. This enabled titrations to be performed in which successively higher deuteroporphyrin concentrations produced a smooth progression in quenching of protein fluorescence. The data in Figure 3 revealed that, for both ChlH and BchH proteins and with both deuteroporphyrin and Mg deuteroporphyrin ligands, quantitative analyses of deuteroporphyrin binding consistently gave satisfactory fits to a single-site binding model. The data show that BchH has a K_d for deuteroporphyrin 2-fold lower than ChlH, indicating a higher affinity for this ligand. Although Mg^{2+} and ATP have little effect on porphyrin binding to BchH, they elevate the K_d more than 3-fold in the case of ChlH. This may reflect allosteric binding of $MgATP^{2-}$, which could have some significance for the proposed regulatory role of the H subunit in chlorophyll biosynthesis and photosynthetic membrane assembly (*13*, *23*). As pointed out in the Introduction, the Mg chelatase H subunits from both *Synechocystis* and *Rb. sphaeroides* were studied because of the contrasting requirements of these organisms for tetrapyrroles. In S*ynechocystis* the flux down the Fe^{2+} branch of tetrapyrrole biosynthesis is expected to be far more significant than in *Rhodobacter*. Undoubtedly, these differences cannot be accounted for solely by in vitro measurements of K_d values for H−porphyrin binding, but the consistently lower values for BchH compared to ChlH could be a contributing factor to partitioning of protoporphyrin at this branch point in tetrapyrrole biosynthesis in a way that favors the chlorophyll branch.

The excitation spectra in Figure 7 show that excitation of aromatic residues in the H proteins elicits a small but measurable fluorescence from bound porphyrin. This is consistent with a recent demonstration that Mg chelatase activity could be reconstituted using the H, I, and D proteins from *Rb. capsulatus*, in which it was reported that excitation of Trp residues in the H subunit could elicit fluorescence from bound porphyrin (*16*). The emission peak of Trp

residues (350 nm) overlaps with the B absorbance band of a bound deuteroporphyrin (392 or 394 nm). Furthermore, the presence of several Trp residues (17 in ChlH, 13 in BchH) means that many or all of them will be at a suitable distance from the porphyrin for resonance energy transfer (~60−70 Å), notwithstanding the large size of the Mg chelatase H subunit. The quenching of H protein fluorescence by added deuteroporphyrin can therefore arise from the presence of bound porphyrin as a "sink" for energy of Trp residues in an excited state, or at the other extreme the quenching could arise from a rearrangement or alteration in conformation of the protein following or accompanying the binding event. At present it can be assumed that both of these mechanisms contribute to the fluorescence quenching. It will be necessary to find independent evidence for an alteration in protein conformation.

Formation of an H−Deuteroporphyrin Complex: Effects on the Spectroscopic Properties of the Porphyrin. The binding of deuteroporphyrin to the H subunit has measurable effects on the spectroscopic properties of the porphyrin. The red shifts of up to 9 nm seen in the B and Q bands of the absorbance spectra in Figure 5, which are also manifested in the emission spectra and excitation spectra, are consistent with nonplanar distortion of the macrocycle, as discussed by Shelnutt et al. (*19*). They found that red shifts were more pronounced for the Q than for the B bands, as we have also seen for the deuteroporphyrin−ChlH and deuteroporphyrin−BchH complexes (Figure 5). There is a relationship between the size of the red shift and the magnitude of distortion; the extent of the shift is relatively insensitive to the distortion of the macrocycle for low and moderate degrees of nonplanarity and then rises more steeply for subsequent increases in distortion (*20*, *21*). The limited extent of the shifts observed in Figure 5 leads to the conclusion that only a small distortion has occurred. It is possible that occupation of a binding site on the H subunit by deuteroporphyrin induces such a distortion in the ligand or accommodates it. It is also possible that this event is associated with an alteration in the conformation of the H protein. Distortion of the porphyrin macrocycle might be required to accommodate the Mg^{2+} ion in a manner similar to the nonplanar distortions of porphyrin observed for ferrochelatase using resonance Raman spectroscopy (*22*). The application of this technique will provide more evidence for similar alterations to the deuteroporphyrin when bound to the H subunit.

Implications for the Catalysis of Mg^{2+} Insertion into Porphyrin. Earlier studies of the lag preceding steady-state chelation had shown that preincubation of ChlH with protoporphyrin, Mg^{2+}, and ATP was effective in decreasing the extent of this lag (*8*), and on the basis of these studies, it was suggested that the H−porphyrin complex is the substrate for Mg chelatase. This model is shown in the reaction scheme above. However direct binding of porphyrin to the H subunit was not shown (*8*). We have shown here that porphyrin can bind to the free H subunit, which is consistent with the model proposed. The gel filtration data suggest monomeric H−porphyrin complexes, for both ChlH and BchH. We propose that the catalytically active H−porphyrin complex is a monomer and that the promotion of this state by porphyrin, ATP, and/or Mg^{2+} was responsible for reducing the lag phase in the chelation reaction (*8*). The K_m for deuteroporphyrin was measured as 8 ± 1.6 μM, and the K_d for deuteroporphyrin is 4.0 ± 1.3 μM for ChlH. It is not possible to say whether these porphyrin binding sites are filled before or during the possibly transient encounter with the I−D−MgATP complex (*9*−*11*). Indeed alternative models where the H subunit remains tightly associated with the ID complex and this complex transiently encounters porphyrin cannot be ruled out on the basis of this or previous work (*8*−*11*). We conclude that the proposal that the H−porphyrin complex is a substrate of Mg chelatase has not been unequivocally demonstrated but that the data we present here are consistent with such a scheme.

The protein fluorescence titration data using Mg−deuteroporphyrin as the ligand provide an insight into the events following Mg^{2+} insertion. It is not known if the Mg−protoporphyrin product dissociates from the H subunit after Mg^{2+} insertion. For example, an H−Mg protoporphyrin complex, rather than the free Mg porphyrin, could be the substrate for the next enzyme in the chlorophyll biosynthetic pathway, Mg−protoporphyrin methyltransferase (EC 2.1.1.11). Therefore, it was of interest to see if Mg−deuteroporphyrin could form a complex with either ChlH or BchH. In each case a complex could be formed, with K_d values similar to those for deuteroporphyrin. The K_d for ChlH−Mg−deuteroporphyrin is approximately 2-fold higher than the corresponding K_d for ChlH−deuteroporphyrin. In contrast, in the case of BchH, the K_d for the product is lower than that for the substrate of the Mg−chelatase reaction. In both cases there was a small increase in the K_d in the presence of $MgATP^{2-}$. These data are consistent with an H−Mg protoporphyrin complex as the substrate for the next enzyme in the chlorophyll biosynthetic pathway, Mg−protoporphyrin methyltransferase; however, more work will have to be carried out, using purified components for both the Mg chelatase and the methyltransferase, to investigate this possibility. This suggestion would also be consistent with the observations of Hinchigeri et al. (*24*) that addition of cell-free extracts of *E. coli* overexpressing *bchH* stimulates the activity of cell-free extracts of *E. coli* containing Mg−protoporphyrin methyltransferase. A linkage between the Mg chelation and methyltransferase steps was suggested many years ago by Gorchein (*25*), who proposed a multienzyme complex for the conversion of protoporphyrin into Mg−protoporphyrin monomethyl ester. This possibility of a direct connection between the two enzymes can now be investigated quantitatively using purified components, with implications for the regulation of the chlorophyll biosynthetic pathway.

REFERENCES

1. Walker, C. J., and Willows, R. D. (1997) *Biochem. J. 327*, 321−333
2. Al-Karadaghi, S., Hansson, M., Nikonov, S., Jönsson, B., and Hederstedt, L. (1997) *Structure 5*, 1501−1510
3. Lecerof, D., Fodje, M., Hansson, A., Hansson, M., and Al Karadaghi, S. (2000) *J. Mol. Biol. 297*, 221−232
4. Gibson, L. C. D., Willows, R. D., Kannangara, C. G., von Wettstein, D., and Hunter C. N. (1995) *Proc. Natl. Acad. Sci. U.S.A. 92*, 1941−1944
5. Jensen, P. E., Gibson, L. C. D., Henningsen, K. W., and Hunter, C. N. (1996) *J. Biol. Chem. 271*, 16662−67
6. Petersen, B. L., Jensen, P. E., Gibson, L. C. D., Stummann, B. M., Hunter, C. N., and Henningsen, K. W. (1997) *J. Bacteriol. 180*, 699−704.

7. Papenbrock, J., Grafe, S., Kruse, E., Hanel, F., and Grimm, B. (1997) *Plant J. 12*, 981−990.
8. Jensen, P. E., Gibson, L. C. D., and Hunter, C. N. (1998) *Biochem. J. 334*, 335−344.
9. Jensen, P. E., Gibson, L. C. D., and Hunter, C. N. (1999) *Biochem. J. 339*, 127−134.
10. Gibson, L. C. D., Jensen, P. E., and Hunter, C. N. (1999). *Biochem. J. 337*, 243−251.
11. Jensen, P. E., Reid, J. D., and Hunter, C. N. (2000) *Biochem. J. 352*, 435−441.
12. Papenbrock, J., Mock, H. P., Kruse, E., and Grimm, B. (1999) *Planta 208*, 264−273.
13. Gibson, L. C. D., Marrison, J. L., Leech, R. M., Jensen, P. E., Bassham, D. C., Gibson, M., and Hunter, C. N. (1996) *Plant Physiol. 111*, 61−71
14. Mochizuki, N., Brusslan, J. A., Larkin, R., Nagatani, A., and Chory, J. (2001) *Proc. Natl. Acad. Sci. U.S.A. 98* 2053−2058
15. Cornejo, J., Willows, R. D., and Beale, S. I. (1998) *Plant J. 15*, 99−107.
16. Willows, R. D., and Beale, S. I. (1998) *J. Biol. Chem. 273*, 34206−34213
17. Kuzmic, P. (1996) *Anal. Biochem. 237*, 260−273.
18. Dawson, R. M. C., Elliott, D. C., Elliott, W. H., and Jones, K. M. (1986) in *Data for Biochemical Research*, 3rd ed., Clarendon Press, Oxford, U.K.
19. Shelnutt, J. A., Song, X.-Z, Ma, J.-G., Jia, S.-L., and Medforth, C. J. (1998) *Chem. Soc. Rev. 27*, 31−41.
20. Jentzen, W., Simpson, M. C., Hobbs, J. D., Song, X., Ema, T., Nelson, N. Y., Medforth, C. J., Smith, K. M., Veyrat, M., Mazzanti, M., Ramasseul, R., Marchon, J.-C., Takeuchi, T., Goddard, W. A., and Shelnutt, J. A. (1995) *J. Am. Chem. Soc. 117*, 11085−11097.
21. Song, X.-Z., Jentzen, W., Jia, S.-L., Jaquinod, L., Nurco, D. J., Medforth, C. J., Smith, K. M., and Shelnutt, J. A. (1996) *J. Am. Chem. Soc. 118*, 12975−12988.
22. Blackwood, M. E., Rush, T. S., Romesberg, F., Schultz, P. G., and Spiro, T. G. (1998) *Biochemistry 37*, 779−782.
23. Hudson, A., Carpenter, R., Doyle, S., and Coen, E. S. (1993) *EMBO J. 12*, 3711−3719.
24. Hinchigeri, S. B., Hundle, B., and Richards, W. R. (1997) *FEBS Lett. 407*, 337−342.
25. Gorchein, A. (1972) *Biochem. J. 127*, 97−106.

BI010562A